Anion Photoelectron Spectroscopy of Vanadium-Doped Cobalt Clusters

Axel Pramann, Kiichirou Koyasu, and Atsushi Nakajima*

Department of Chemistry, Faculty of Science and Technology, Keio University, 3-14-1 Hiyoshi, Kohoku-ku, Yokohama 223-8522, Japan

Koji Kaya

Institute of Molecular Science, Myodaiji, Okazaki 444-8585, Japan

Received: October 11, 2001; In Final Form: December 11, 2001

Bimetallic cobalt (Co)−vanadium (V) clusters, $Co_nV_m^-$ ($n = 4-14$, $m = 0-2$), are investigated using anion photoelectron spectroscopy at 4.66 eV photon energy. Electron affinities (EA) and vertical detachment energies (VDE) are determined, and the electronic structures of V- and V_2-doped Co_n clusters are compared to those of pure Co_n clusters. Bonding and hybridization effects can be explained using a charge-transfer model. A peak shape analysis confirms the high stability of the $Co_{12}V$ cluster with a most plausible icosahedral structure with the V atom in the cage center. Together with ionization potentials (IP), the electronic structures of the clusters are compared to H_2 chemisorption rate coefficients reported previously. Thus, this study completes the investigation of electronic properties and reactivity of the bimetallic Co_nV_m clusters as a function of charge, size, and distribution. Although the reactivity of Co_nV_m reveals a better correlation toward the EA rather than toward IP, no improved correlation is found between promotion energies and reactivity. This result clearly shows that the chemisorption reactivity of the heterogeneous clusters is largely governed by geometric factors.

Introduction

In recent years, bimetallic clusters have become a matter of increasing interest in cluster research (see, for example, refs 1−5). The reason for this development is evident: when doping pure metals or metal surfaces with metallic heteroatoms, the new system often exhibits more tailored properties for applications than the nondoped pure metals.[6,7] One central area of application is heterogeneous catalysis; enhanced catalytic activity and selectivity is often gained by using doped bimetallic catalysts.[8,9]

The investigation of bimetallic or alloy clusters provides a state-of-the-art tool to gain insights into chemical and physical properties of bimetallic systems on a microscopic scale (e. g., geometric and electronic structures) as a function of size and distribution. These structures can be compared and sometimes correlated with size-dependent chemical reaction rates and other important properties. Only a number of studies have been performed during the last years to examine such kinds of structure/reactivity correlations. One example is the correlation between ionization potentials (IP) and hydrogen chemisorption rates of Fe_n clusters.[10] Also a direct relation between D_2 reaction rates of Nb_n clusters and their corresponding ionization threshold energies has been observed.[11] In the case of Fe_n, Co_n, and Ni_n clusters, a correlation has been found between the IP/EA difference and H_2 chemisorption rates as an analogy to solid surfaces.[12] This method has also been successfully applied to pure Nb_n clusters by Gantefoer and Eberhardt and co-workers,[13] and recently to Al-doped Nb_n clusters by our group.[14] Nevertheless, electronic factors share the responsibility of a size-selective reactivity more or less with geometric factors as has been pointed out by Knickelbein[15] in the case of the H_2 chemisorption behavior of bimetallic aluminum/cobalt clusters. These examples indeed show that the combination of different size-dependent properties help to understand the chemical and physical behavior of small gas-phase bimetallic clusters in more detail.

In the current paper, we report for the first time on the investigation of the size-dependent evolution of the electronic structure of bimetallic Co_nV^- ($n = 3-13$) and $Co_nV_2^-$ ($n = 7-12$) clusters with the aid of anion photoelectron spectroscopy using a fixed photon energy of 4.66 eV. The main objective of this study is the examination of the electronic structures of these small clusters as a function of cluster size and distribution. Additionally, the electronic structures of the $Co_nV_m^-$ bimetallic clusters are compared to pure Co_n^- clusters, which we have measured under the same experimental conditions. The nature of chemical bonding in the $Co_nV_m^-$ clusters is explained using a charge-transfer model. Hybridization effects between the Co_n^- clusters and the V atoms are discussed. The electronic structures of the Co_nV_m clusters are compared to chemisorption rate coefficients of the reactions of neutral Co_nV_m clusters toward H_2, which have been reported by our group earlier.[16−18] Applying a frontier orbital approach using promotion energies, a reactivity/electronic structure correlation has been investigated, which can be applied for the Co_n and tentatively for $Co_{n-1}V_1$ clusters for $n > 9$ except $n = 13$, but not for the $Co_{n-2}V_2$ cluster series.

Experiment

The experimental apparatus and applied methods have been reported in detail elsewhere.[16,19] Therefore, only a brief description will be given. Generation of bimetallic $Co_nV_m^-$ cluster anions is performed as follows. Two independently operating Nd^{3+}:YAG lasers (532 nm) are focused onto a rotating and translating Co rod (downstream location) and a V rod (upstream location), respectively. Then, clusters are formed by cooling

* Corresponding author. Fax: +81-45-566-1697. E-mail: nakajima@sepia.chem.keio.ac.jp.

10.1021/jp013791f CCC: $22.00
Published on Web 02/26/2002

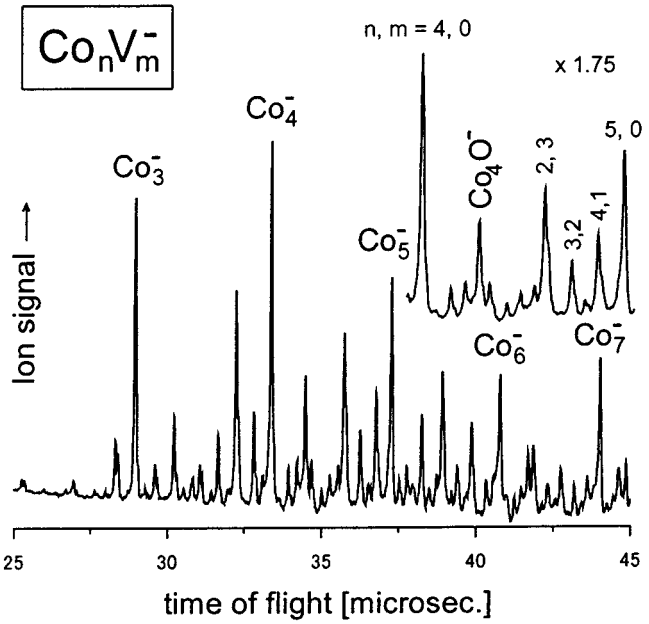

Figure 1. A part of a time-of-flight mass spectrum of $Co_nV_m^-$. clusters. In the enlarged inset, the typical distribution of V_m-doped Co_n^- clusters is shown in more detail. Bimetallic $Co_nV_m^-$ clusters reveal three main series: $Co_{n-1}V^-$, $Co_{n-2}V_2^-$, and $Co_{n-3}V_3^-$. Pure Co_n^- clusters are accompanied by Co_nO^- peaks.

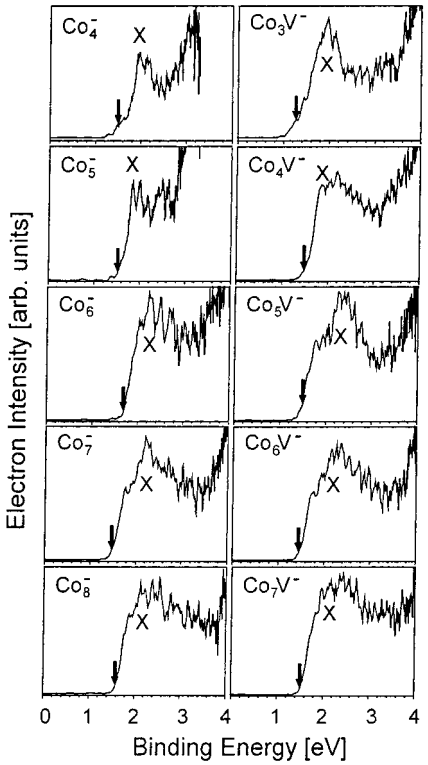

Figure 2. Photoelectron spectra of pure Co_n^- clusters (left column: $n = 4-8$, at 3.49 or 4.66 eV) and bimetallic $Co_{n-1}V_1^-$ clusters (right column: $n = 4-8$, at 4.66 eV). The spectra of Co_n^- correspond well to those reported in ref 26. EA values are indicated by downward arrows (for details, see text).

the plasma with a high-pressure helium pulse (10 atm stagnation pressure) in a 2 mm diameter channel of 20 mm length. After a supersonic expansion the clusters are mass-analyzed by their *m*/*z* ratio with an in-line time-of-flight mass spectrometer (TOF-MS) having a resolution of $m/\Delta m = 230$. To decrease the amount of energy broadening of the photoelectron spectra caused by the Doppler effect, the mass-selected cluster anions are decelerated with a special deceleration technique originally reported by Handschuh et al.[20] In the center of the magnetic bottle-type time-of-flight photoelectron spectrometer (TOF-PES)[21−23] the clusters are irradiated with the fourth harmonics output (4.66 eV) of a Q-switched Nd^{3+}:YAG laser (laser fluence: 1−2 mJ/cm^2). The kinetic energies of the detached electrons are measured by their time-of-flight, and electron kinetic energy spectra are converted to the electron binding energy spectra by subtracting the kinetic energy from the photon energy. The TOF-PES is calibrated using the strong line of the ground-state transition ($^1S_0 \rightarrow {}^2S_{1/2}$) of the gold atomic anion.[24] The resolution of the spectrometer is better than 50 meV at 1 eV electron kinetic energy (eKE), and decreases according to $(eKE)^{3/2}$ at higher kinetic energies. In the current experiment, photoelectron (PE) spectra are measured by accumulating 10000−30000 experimental runs at 10 Hz repetition rate. During all measurements, the PE spectral shapes do not reveal any laser-power-dependent changes.

Results and Discussion

A. Mass Spectra of $Co_nV_m^-$. Figure 1 shows a part of a typical time-of-flight mass spectrum of $Co_nV_m^-$ clusters in the size range $n = 3-7$. The pure Co_n^- clusters have higher intensities than the corresponding bimetallic clusters showing a maximum at Co_4^-. Due to the high reactivity of cobalt, which is an open d-shell transition metal with a $[Ar]3d^74s^2$ atomic electron configuration, the pure Co_n^- clusters are always accompanied by monoxide peaks of Co_nO^-, even when operating under carefully clean source conditions. The enlarged inset shows in more detail the distribution of the bimetallic $Co_nV_m^-$ clusters: At least three different series of $Co_nV_m^-$ clusters can be observed which appear on the low mass side of each Co_n^- cluster: $Co_{n-1}V^-$, $Co_{n-2}V_2^-$, and $Co_{n-3}V_3^-$. A first observation is that the distribution of the *negatively* charged $Co_nV_m^-$ clusters is exactly the same as that of the corresponding neutral and cationic clusters, which are reported in refs 16 and 17. Since the distribution is charge independent, this qualitatively implies a substantial geometric influence on the bimetallic clusters.

B. Photoelectron Spectra of $Co_nV_m^-$ Clusters. Photoelectron spectra of $Co_nV_m^-$ clusters are measured at 4.66 eV photon energy (see Figures 2 and 3). According to the one particle approximation, the entire photodetachment process can be described as electronic transitions from the ground state of the negatively charged cluster to the ground or excited states of the corresponding neutral cluster in the geometry of the anion. During the transition, the total spin can change only by 1/2. Usually, a broadening of the signals indicates a geometry change between the anion and the neutral cluster after photodetachment as a result of Franck−Condon factors for the respective transitions. In the current study, threshold energies are determined from the intersection of a straight line on the slope of the first intense peak with the binding energy axis or by taking the binding energy at 5% of the first peak maximum. The threshold energies are defined as upper limits of adiabatic EA and thus in the following named as EA, although adiabatic EA can only be determined when the $0 \leftarrow 0$ ground-state transition is resolved. Additionally, vertical detachment energies (VDE) are determined from the maxima of the PE peaks. EA and VDE values of Co_nV_m clusters are listed in Table 1. In Figure 4, EA values are displayed with IPs reported previously.[18,25] Furthermore, EA values are plotted together with relative rate coefficients (rc) of H_2 chemisorption reactions of neutral clusters in Figure 5. The latter are discussed in subsection B.3.

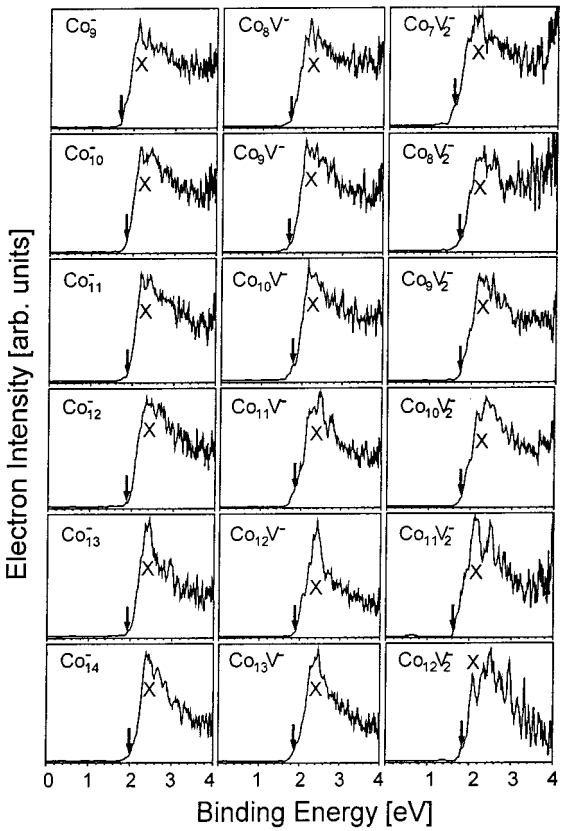

Figure 3. Photoelectron spectra of pure Co_n^- clusters (left column: $n = 9-14$, at 4.66 eV), $Co_{n-1}V_1^-$ clusters (center column: $n = 9-14$, at 4.66 eV), and $Co_{n-2}V_2^-$ clusters (right column: $n = 9-14$, at 4.66 eV). The spectra of Co_n^- correspond well to those reported in ref 26. EA values are indicated by downward arrows (for details, see text).

TABLE 1: Electron Affinities (EA) and Vertical Detachment Energies (VDE) of Co_nV Clusters ($n = 3-13$) and Co_nV_2 Clusters ($n = 7-12$)[a]

cluster size (n, m)	EA [eV]	VDE [eV]
3, 1	1.28(19)	1.96(20)
4, 1	1.54(23)	1.85(18)
5, 1	1.60(24)	2.26(22)
6, 1	1.44(21)	2.15(21)
7, 1	1.54(23)	2.17(21)
8, 1	1.74(26)	2.17(21)
9, 1	1.71(25)	2.08(20)
10, 1	1.83(27)	2.15(21)
11, 1	1.88(28)	2.45(24)
12, 1	1.93(29)	2.43(24)
13, 1	1.94(29)	2.47(24)
7, 2	1.60(24)	2.03(20)
8, 2	1.77(26)	2.26(22)
9, 2	1.77(26)	2.17(21)
10, 2	1.85(27)	2.15(21)
11, 2	1.74(26)	2.13(21)
12, 2	1.88(28)	2.08(20)

[a] Uncertainties are given in parentheses (1.60(24) eV means 1.60 ± 0.24 eV).

B.1. $Co_{n-1}V_1^-$. The PE of pure Co_n^- clusters (left columns) and bimetallic $Co_{n-1}V_1^-$ clusters (right and center columns) are shown in Figures 2 and 3. We have measured the PE spectra of pure Co_n^- clusters under the same experimental conditions to provide a direct comparison of the electronic structures of pure and vanadium-doped Co_n clusters. Pure Co_n^- clusters reveal the same spectral features as reported in the work of Kondow and co-workers.[26] In the spectra, the downward arrows indicate EA, and the first VDE values are marked with X corresponding to transitions from the ground state of the anion to the ground state of the neutral. As has been reported,[26] only very small

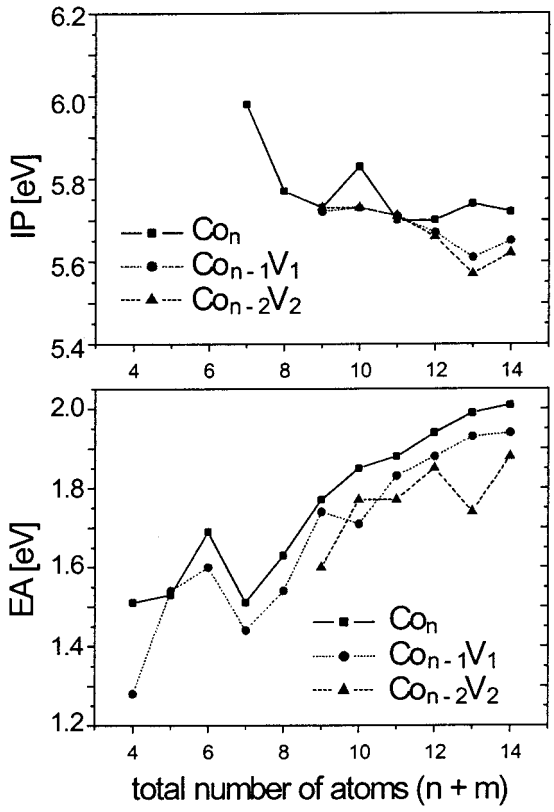

Figure 4. Upper plot: ionization potentials (IP) of Co_n (solid squares, from ref 25), $Co_{n-1}V_1$ (solid circles, from ref 18), and $Co_{n-2}V_2$ (solid triangles, from ref 18). Lower plot: electron affinities (EA) of Co_n (solid squares), $Co_{n-1}V_1$ (solid circles), and $Co_{n-2}V_2$ (solid triangles). For more clarity, error bars are not displayed (see Table 1).

Co_n^- clusters ($n > 6$) exhibit some distinct structures. Already from $n = 6$ the spectral features become very similar and only the threshold binding energy is shifted to higher values with increasing cluster size. The reason for the structureless pattern of Co_n^- clusters is the high density of low lying electronic states in a small energy range above the threshold. For a better resolution, we have measured the PE spectra of Co_4^- and Co_5^- with the third harmonics output of the Nd^{3+}:YAG laser (3.49 eV). For Co_4^- a sharp peak evolves at 2 eV resulting from Co 4s-derived states. The influence of 3d-derived states is already very strong at $n = 4$, and a complete merging of 4s- and 3d-derived states of Co appears at $n = 5$. Thus, the Co_n^- spectra for $n > 6$ reveal broad features which are attributed to 3d-derived states. With increasing n, the electronic structure of pure Co_n^- approaches that of bulk phase cobalt and the spectral features become very similar. This structural transition is estimated to evolve around $n = 7$ when applying the conducting spherical droplet (csd) model.[26]

At $n = 13$, the PE spectrum shows a sharp peak which most probably results from a rigid spherical geometry of a perfect icosahedron (I_h). In several cases, the 13-mer cluster reveals a high ionization potential due to a high and rigid geometric structure and the presence of very stable isomers as has been pointed out for Mn_{13} by Nayak et al.[27] Moreover, the geometry of the neutral Co_{13} cluster has been determined to a cubic-based (fcc/hcp) structure with the aid of a chemical probe experiment.[28]

The IP values of Co_nV_m in Figure 4 exhibit a local maximum for Co_{13}, but local minima for $Co_{12}V_1$ and $Co_{11}V_2$, though they are not conspicuous. In the course of the EA values on the other hand, a local minimum is observed only for $Co_{11}V_2$. Thus, no common electronic behavior can be observed at the 13-mer in

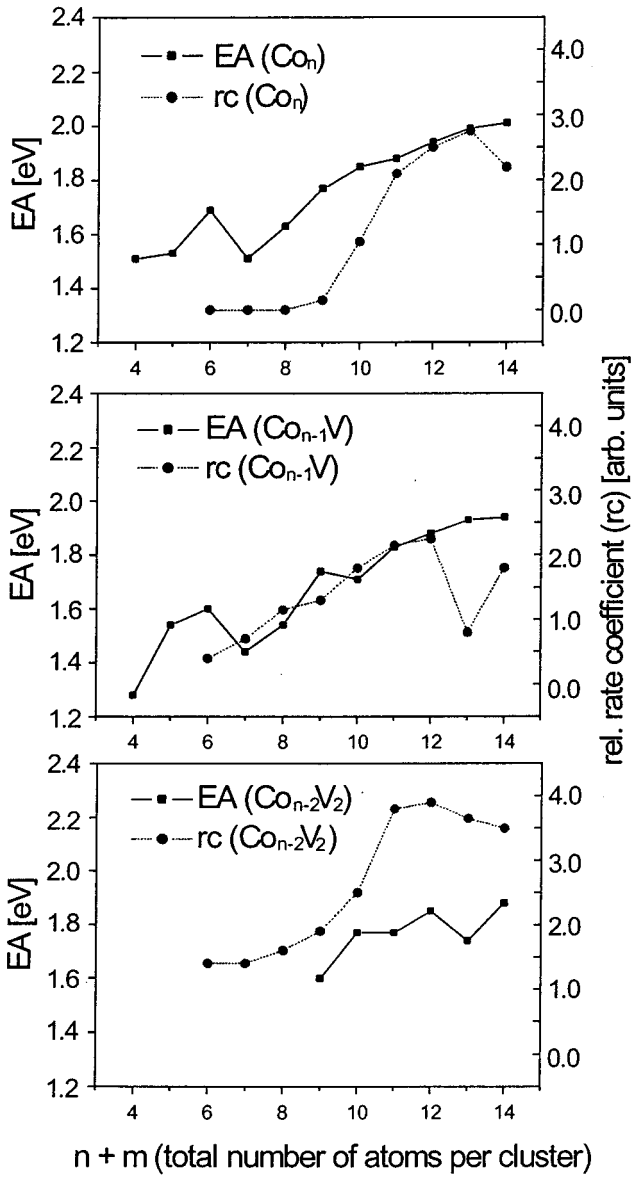

Figure 5. Comparison of electron affinities (EA, solid squares) and relative rate coefficients (rc, solid circles, taken from ref 16) as a function of the total number of atoms ($n + m$) of Co_nV_m clusters: upper plot: Co_n; center plot: $Co_{n-1}V_1$; lower plot: $Co_{n-2}V_2$.

terms of size-dependence of EA and IP values. The geometric rigidity will be discussed later in section B.3.

The PE spectra of bimetallic $Co_{n-1}V_1^-$ clusters are shown in the right column of Figure 2 and in the center column of Figure 3, where both were measured at 4.66 eV photon energy. In Figure 2, the spectra of Co_3V^- up to Co_7V^- show some broadening which cannot be attributed to the slightly lower resolution of the 4.66 eV photon energy alone. This broadening of the threshold features is presumably ascribed to a consequence of the hybridization of the Co_n 3d-derived molecular orbitals (MO) and the 3d atomic orbital (AO) of the incoming V atom. When comparing the PE spectra of pure Co_n clusters and $Co_{n-1}V^-$ clusters in the size range $n = 6-13$, it is obvious that the spectral features are very similar: a broad strong peak evolving around 1.5 eV with a tail around 4 eV. Generally, with increasing size the EA values shift to higher values revealing little difference between the pure and V-atom-doped Co_n clusters which is depicted in Figure 4. Only for $n = 6$ the EA difference between the pure and V-atom-doped Co_n clusters is larger (270 meV). This deviation can be explained by the existence of isomers, but a complete understanding is still lacking without the availability of theoretical calculations.

The similarity of the Co_n and the $Co_{n-1}V_1$ spectra from $n > 6$ qualitatively indicates a weak electronic perturbation of the Co_n cluster framework by the incoming V atom. This can be understood when considering that the size of the V 3d orbital (atomic electron configuration of V: $[Ar]3d^34s^2$) is very similar to that of Co 3d- or Co 3d4s-derived frontier orbitals. Thus, an effective overlap of the wave functions results in a similar bonding. Additionally, the Wigner−Seitz radius of Co is similar to that of V (131.1 pm and 125.3 pm, respectively). Therefore, a geometrical change coupled with the electronic structure will be of minor relevance.

Bonding between the Co_n cluster and the V atom can be explained using a frontier orbital approach.[29,30] In this picture, the valence MOs of the Co_n cluster interact with AOs of the V atom resulting in a new set of bonding and antibonding MOs. In the initial step, electron transfer occurs from the vanadium 4s AO into a 3d-derived LUMO (LUMO: the *L*owest *U*noccupied *M*olecular *O*rbital) of the respective neutral Co_n cluster. This direction of the charge transfer can be understood as a result of the difference in electronegativities (EN(Co) = 1.7, EN(V) = 1.5). Then, back-donation of an electron from the Co_n 3d-derived HOMO level (HOMO: the *H*ighest *O*ccupied *M*olecular *O*rbital) to an empty V 3d AO leads to the stabilization of the Co−V bond. For pure Co_n^- clusters a nearly free electron metallic-like bonding is postulated for $n > 7$.[26] The similarity of the PE spectra of pure and V-doped Co_n clusters also suggests a similar kind of metallic-like bonding, which is somewhat different from that of main-group metal/transition metal bimetallic clusters (see, for example, $Al_nCo_m^-$ (ref 31)).

When one Co atom in the Co_n^- cluster is substituted by a V atom resulting in a bimetallic cluster of $Co_{n-1}V_1^-$, the electronic structure will not change greatly: the most stable oxidation states of atomic Co are +2 and +3 ($3d^7$ and $3d^6$, respectively). These oxidation states can be maintained also by the V atom ($3d^3$ and $3d^2$, respectively), though V is possibly a stronger electron donor with the most stable oxidation state of +5 ($3d^0$). Using this picture, we can understand the very similar electronic structure of pure and V-doped Co_n clusters in a first attempt, even though accurate calculations concerning the electronic structure are needed. In Figure 4, both EA and IP values of Co_n, $Co_{n-1}V_1$, and $Co_{n-2}V_2$ clusters are plotted versus the total number of atoms per cluster. The IPs are taken from refs 18 and 25. Indeed both EA and IP values of pure Co_n clusters show no special size dependence for $n > 10$. At infinite size, both EA and IP values will merge at the bulk work function of the Co_nV_m system.

B.2. $Co_{n-2}V_2^-$. The PE spectra of the $Co_{n-2}V_2^-$ clusters ($n = 9-14$) are shown in the right column of Figure 3. Due to poor ion intensities compared to pure and single V-doped Co_n^- clusters, the spectra reveal lower signal-to-noise ratios, especially at electron binding energies above 3 eV. The $Co_{n-2}V_2^-$ clusters show also very similar features as can be observed in those of the $Co_{n-1}V_1^-$ clusters: a broad strong feature arising near the threshold with a tail between 3 and 4 eV. The course of threshold energies (EAs) of $Co_{n-2}V_2$ displayed in Figures 3 and 4 is quite similar to that of $Co_{n-1}V_1$ except of $n = 13$. An interesting feature arises at $Co_{11}V_2^-$: here, the first intense peak reveals a splitting by 400 meV, indicating the prominent influence of a second V atom. In the icosahedral structure, the second V atom cannot be hosted inside a Co cage. Although a vibrational interaction with the Co cage might cause a more structured feature in the threshold energy region, the most plausible explanation for the splitting is the coexistence of two structural

isomers. Here, two isomers are conceivable. One structure is that having one central V atom and one surface V atom, and the other is that having two surface V atoms. Although it is not possible to assign which isomers exhibit a low EA by experiments only, the spectral sharpness due to the rigidity can plausibly reveal the coexistence of isomers.

B.3. Comparison of Electronic Structures and Hydrogen Chemisorption Rates. The chemisorption rate behavior of neutral Co_nV_m clusters toward H_2 has been reported in detail.[16] In brief, after doping the Co_n clusters with V_m ($m = 1-3$), the chemisorption rate coefficients (relative reactivities) increase drastically for $n = 5$, 7, and 9, compared to pure Co_n clusters. The most interesting feature is the extremely low reactivity of $Co_{12}V$ toward H_2 compared to neighbored cluster sizes. A plausible explanation of this special size-selective behavior of $Co_{12}V$ is its special rigid geometry: an icosahedron with an active V atom in the center shielded against the interaction with H_2.[16,31] After the addition of a second V atom the reactivity sharply increases because of the surface position of the new incoming V atom which acts as a reactive site toward H_2.

In Figure 5, EA values of Co_nV_m ($m = 0-2$) are displayed together with relative rate coefficients of the respective neutral clusters reported in ref 16. As already discussed, the addition of one or two V atoms to a Co_n cluster does not significantly change the PE spectra. When comparing EA values and rate coefficient (rc) values, a better correlation is found between them rather than between IP and rc values.[18] However, the reactivity enhancement by the V-doping cannot be explained by the EA change at all. Thus, the statement[16] of geometric effects as the driving force for an increase of reactivity seems reasonable. In that case, the doping of V atoms into the nonreactive Co_n cluster induces reactive sites due to a different geometry and surface perturbation. But the extraordinary stability of the $Co_{12}V$ cluster toward H_2 also reveals electronic arguments: comparing the PE spectra of Co_{12}^- and $Co_{12}V^-$ (Figure 3) the first peak is more sharp than in the spectrum of the nondoped cluster. Figure 6 shows the experimental PE spectra of Co_{12}^-, $Co_{12}V^-$, and Co_{13}^- (solid lines). Comparing the spectra of $Co_{12}V^-$ and Co_{13}^-, it is evident that both show a very similar electronic structure. The geometric structure of $Co_{12}V^-$ can be described by a Co_{12}^- cluster with an incorporated V atom which is shielded against H_2 chemisorption. The dotted lines show Gaussian fits in the energy range between 1.9 and 2.8 eV. The best fit is obtained for $Co_{12}V^-$ where the intracluster vibrations and thus spectral broadening are comparably reduced due to the central V atom of the $Co_{12}V$ icosahedron. On one hand, a small geometry change and larger Franck−Condon factors for the ground-state transition are evident. On the other hand, electronic stabilization might be contributed from an electronic shell effect:[32] each Co atom can contribute 3 valence electrons (final state: d^6) as well as the V atom (final state: d^2). Since the stable Al_{13}^- appears due to a closed electronic shell with 40 electrons, the similar electronic shell closing is completed by $Co_{12}V^-$ ($36 + 3 + 1 = 40$ electrons) and by Co_{13}^-.

Additionally, we have determined promotion energy (EP) values for $Co_{n-1}V_1$ and $Co_{n-2}V_2$ which are displayed in Figure 7 together with relative rate coefficients of the H_2 chemisorption reaction. Briefly, the EP is defined as the energy required to promote an electron from an occupied frontier orbital of a cluster to one of the more localized unoccupied frontier orbitals. The promotion energy (EP) is calculated by the following equation: $EP(n) = IP(n) - EA(n) - e^2/R(n)$ with $R(n)$ as the respective cluster radius, and the electronic charge e. Originally applied for metal surfaces, a chemisorption/electronic structure correlation model has been successfully applied to pure metal clusters by Smalley and co-workers.[12] In that model the cluster reactivity

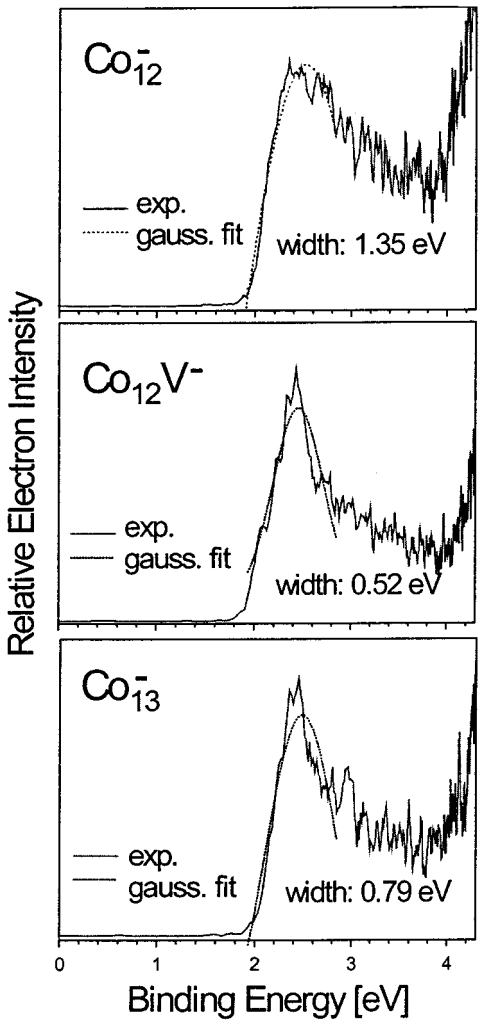

Figure 6. Photoelectron spetra of Co_{12}^-, $Co_{12}V^-$, and Co_{13}^- (solid lines) at 4.66 eV. The peak shape of the first VDE is analyzed with a Gaussian-type fitting function (for details, see text). The geometry change in the vertical transition is minor for $Co_{12}V^-$.

is strongly dependent on the height of an entrance channel barrier caused by the Pauli repulsion between the cluster and the incoming H_2 molecule. The barrier is proportionial to the respective promotion energy. In ref 12 this approach works very well in the case of pure Fe, Ni, and Co clusters. The correlation for Co_n clusters is displayed in the top of Figure 7. Within the experimental error, a correlation of relative rate coefficients and EP values is observed for Co_n ($n > 9$), which matches considerably well with that reported in ref 12. For $Co_{n-1}V_1$ a similarity in the curvature of the EP and rc data is obvious for $n > 9$ except $n = 13$. This is a surprising observation, since in the calculations of Fujima and Yamaguchi[33] the electronic structure effect upon the H_2 chemisorption behavior of Co_{13}, $Co_{12}V$ has been clearly demonstrated. This reveals a possible limitation of the promotion energy/reactivity correlation approach in the case of heterogeneous clusters hosting a heteroatom in the cage center, which cannot interact with the frontier orbitals of small molecules. For pure clusters the reaction probability is only determined by the size and not by the distribution. For $Co_{n-2}V_2$, however, a correlation cannot be observed at all.

The chemisorption pattern of positively charged $Co_nV_m^+$ toward H_2 has also been reported.[17] That study focuses on H_2 chemisorption rates of $Co_{n-m}V_m^+$ ($n = 2-19$) and a strong charge effect toward reactivity behavior due to the localization of the positive charge has been found: Only for $n = 4$ and 5

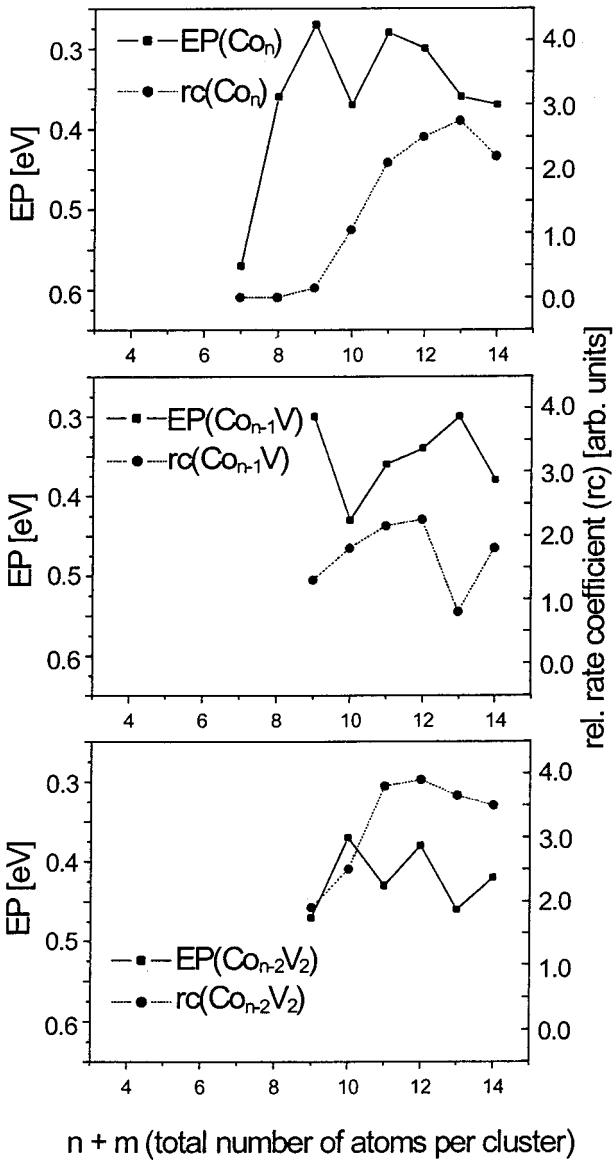

Figure 7. Comparison of promotion energies (EP, solid squares) and relative rate coefficients (rc, solid circles, taken from ref 16) as a function of the total number of atoms ($n + m$) of Co_nV_m clusters: upper plot: Co_n; center plot: $Co_{n-1}V_1$; lower plot: $Co_{n-2}V_2$.

does a strong increase in reactivity appear. For larger clusters ($n > 13$) the single V substitution leads to a reactivity decrease and the substitution with a second V atom slightly increases the reactivity. $Co_{12}V^+$ also shows a low reactivity toward H_2 similar as the neutral cluster. All these reactivity changes have been attributed to geometric reasons. For the heterogeneous bimetallic clusters, particularly, the main driving force for size-dependent reactivity is closely related to the change of the geometric structures even when an electronic contribution is evident for special cluster sizes.

Conclusions

Photoelectron spectra of bimetallic $Co_{n-1}V_1^-$ ($n = 4-14$) and $Co_{n-2}V_2^-$ ($n = 9-14$) clusters have been investigated using anion photodetachment photoelectron spectroscopy at 4.66 eV photon energy in a molecular beam experiment. The evolution of the electronic structure as a function of cluster size and distribution is studied, and EA and VDE values are determined. The size-dependent electronic structure is compared to H_2 chemisorption rates of the corresponding neutral clusters. A similarity in the curvature of EP and rc is found for $Co_{n-1}V_1$ ($n > 9$), except $n = 13$, but not for the $Co_{n-2}V_2$ cluster series. Thus, corresponding to postulations of earlier works on Co_nV_m clusters, the main driving force for size-selective reactivity is closely related to the cluster geometry.

Acknowledgment. This work is supported by a program entitled "Research for the Future (RFTF)" of the Japan Society for the Promotion of Science (98P01203) and by a grant-in-aid for scientific research (C) (No. 13640582) from the Ministry of Education, Science, Sports and Culture. A.P. gratefully acknowledges a postdoctoral fellowship from the Japan Society for the Promotion of Science (JSPS).

References and Notes

(1) Koretsky, G. M.; Kerns, K. P.; Nieman, G. C.; Knickelbein, M. B.; Riley, S. J. *J. Phys. Chem. A* **1999**, *103*, 1997, and references therein.
(2) Taylor, T. G.; Willey, K. F.; Bishop, M. B.; Duncan, M. A. *J. Phys. Chem.* **1990**, *94*, 8016.
(3) Heiz, U.; Vayloyan, A.; Schumacher, E.; Yeretzian, C.; Stener, M.; Gisdakis, P.; Roesch, N. *J. Chem. Phys.* **1996**, *105*, 5574.
(4) Thomas, O. C.; Zheng. W.; Bowen, K. H., Jr. *J. Chem. Phys*. **2001**, *114*, 5514.
(5) Thomas, O. C.; Zheng, W.-J.; Lippa, T. P.; Xu, S.-J.; Lyapustina, S. A.; Bowen, K. H., Jr. *J. Chem. Phys*. **2001**, *114*, 9895.
(6) *Physical and Chemical Properties of Thin Metal Overlayers and Alloy Surfaces*; Zehner, D. M., Goodman, D. M., Eds.; Mater. Res. Soc. **1987**, 83.
(7) Rodriguez, J. A. *Surf. Sci. Rep.* **1996**, *24*, 223.
(8) Sinfelt, J. H. *Bimetallic Catalysis: Discoveries, Concepts and Applications*; Wiley: New York, 1983.
(9) Koel, B. E.; Somorjai, G. A. In *Catalysis*; Anderson, J. R., Boudart, M., Eds.; Springer-Verlag: Berlin, 1985.
(10) Whetten, R. L.; Cox, D. M.; Trevor, D. J.; Kaldor, A. *Phys. Rev. Lett.* **1985**, *54*, 1494.
(11) Whetten, R. L.; Zakin, M. R.; Cox, D. M.; Trevor, D. J.; Kaldor, A. *J. Chem. Phys.* **1986**, *85*, 1697.
(12) Conceicao, J.; Laaksonen, R. T.; Wang, L.-S.; Guo, T.; Nordlander, P.; Smalley, R. E. *Phys. Rev. B* **1995**, *51*, 4668.
(13) Kietzmann, H.; Morenzin, J.; Bechthold, P. S.; Gantefoer, G.; Eberhardt, W. *J. Chem. Phys.* **1998**, *109*, 2275.
(14) Pramann, A.; Nakajima, A.; Kaya, K. *Chem. Phys. Lett.* **2001**, *347*, 366.
(15) Menezes, W. J. C.; Knickelbein, M. B. *Chem. Phys. Lett.* **1991**, *183*, 357.
(16) Nonose, S.; Sone, Y.; Onodera, K.; Sudo, S.; Kaya, K. *J. Phys. Chem.* **1990**, *94*, 2744.
(17) Nakajima, A.; Kishi, T.; Sugioka, T.; Sone, Y.; Kaya, K. *J. Phys. Chem.* **1991**, *95*, 6833.
(18) Hoshino, K.; Naganuma, T.; Watanabe, K.; Konishi, Y.; Nakajima, A.; Kaya, K. *Chem. Phys. Lett.* **1995**, *239*, 369.
(19) Nakajima, A.; Taguwa, T.; Hoshino, K.; Sugioka, T.; Naganuma, T.; Ono, F.; Watanabe, K.; Nakao, K.; Konishi, Y.; Kishi, R.; Kaya, K. *Chem. Phys. Lett.* **1993**, *214*, 22.
(20) Handschuh, H.; Gantefoer, G.; Eberhardt, W. *Rev. Sci. Instrum.* **1995**, *66*, 3838.
(21) Kruit, P.; Read, F. H. *J. Phys. E* **1983**, *16*, 313.
(22) Cheshnovsky, O.; Yang, S. H.; Pettiette, C. L.; Craycraft, M. J.; Smalley, R. E. *Rev. Sci. Instrum.* **1987**, *58*, 2131.
(23) Gantefoer, G.; Meiwes-Broer, K. H.; Lutz, H. O. *Phys. Rev. A* **1988**, *37*, 2716.
(24) Hotop, H.; Lineberger, W. C. *J. Phys. Chem. Rev. Data* **1975**, *4*, 539.
(25) Yang, S.; Knickelbein, M. B. *J. Chem. Phys.* **1990**, *93*, 1533.
(26) Yoshida, H.; Terasaki, A.; Kobayashi, K.; Tsukada, M.; Kondow, T. *J. Chem. Phys.* **1995**, *102*, 5960.
(27) Nayak, S. K.; Nooijen, M.; Jena, P. *J. Phys. Chem. A* **1999**, *103*, 9853.
(28) Riley, S. J. *J. Non-Cryst. Solids* **1996**, *205*−*207*, 781.
(29) Saillard, J.-Y.; Hoffman, R. *J. Am. Chem. Soc.* **1984**, *106*, 2006.
(30) Hoffman, R. *Solids and Surfaces: A Chemist's View of Bonding in Extended Structures*; VCH: Weinheim, 1988.
(31) Pramann, A.; Nakajima, A.; Kaya, K. *J. Chem. Phys*. **2001**, *115*, 5404.
(32) Knight, W. D.; Clemenger, K.; de Heer, W. A. Saunders, W. A.; Chou, M. Y.; Cohen, M. L. *Phys. Rev. Lett.* **1984**, *24*, 2141.
(33) Fujima, N.; Yamaguchi, T. *J. Phys. Soc. Jpn.* **1992**, *61*, 1724.